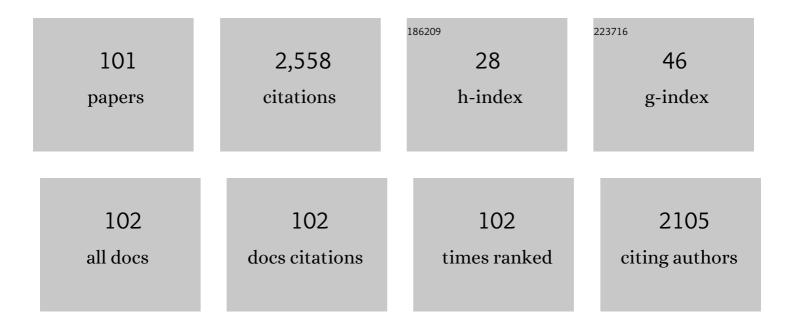
List of Publications by Year in descending order

Source: https://exaly.com/author-pdf/8753343/publications.pdf Version: 2024-02-01



#	Article	IF	CITATIONS
1	A multibranch, multitarget neural network for rapid point-source inversion in a microseismic environment: examples from the Hengill Geothermal Field, Iceland. Geophysical Journal International, 2022, 229, 999-1016.	1.0	8
2	Seismic tremor reveals slow fracture propagation prior to the 2018 eruption at Sierra Negra volcano, Galápagos. Earth and Planetary Science Letters, 2022, 586, 117533.	1.8	4
3	Monitoring microseismicity of the Hengill Geothermal Field in Iceland. Scientific Data, 2022, 9, 220.	2.4	9
4	Understanding Seismic Waves Generated by Train Traffic via Modeling: Implications for Seismic Imaging and Monitoring. Seismological Research Letters, 2021, 92, 287-300.	0.8	18
5	Quantifying strong seismic propagation effects in the upper volcanic edifice using sensitivity kernels. Earth and Planetary Science Letters, 2021, 554, 116683.	1.8	2
6	2D Synthetic dataset of numerical simulations of long-period seismicity in a volcanic edifice and related sensitivity kernels. Data in Brief, 2021, 34, 106673.	0.5	0
7	Caldera resurgence during the 2018 eruption of Sierra Negra volcano, Galápagos Islands. Nature Communications, 2021, 12, 1397.	5.8	30
8	How deep ocean-land coupling controls the generation of secondary microseism Love waves. Nature Communications, 2021, 12, 2332.	5.8	13
9	Preâ€migration diffraction separation using generative adversarial networks. Geophysical Prospecting, 2021, 69, 949-967.	1.0	6
10	North Atlantic Oscillation (NAO) Climate Index Hidden in Ocean Generated Secondary Microseisms. Geophysical Research Letters, 2021, 48, e2021GL093657.	1.5	0
11	Dynamic earthquake triggering response tracks evolving unrest at Sierra Negra volcano, Galápagos Islands. Science Advances, 2021, 7, eabh0894.	4.7	4
12	Deformation-controlled long-period seismicity in low-cohesion volcanic sediments. Nature Geoscience, 2021, 14, 942-948.	5.4	6
13	Characterization and location of flow-induced seismic signals in karst using passive seismic. , 2021, , .		Ο
14	RETREAT: A REal-Time TREmor Analysis Tool for Seismic Arrays, With Applications for Volcano Monitoring. Frontiers in Earth Science, 2020, 8, .	0.8	5
15	Enhancing interpretability with diffraction imaging using plane-wave destruction aided by frequency-wavenumber f-k filtering. Interpretation, 2020, 8, T541-T554.	0.5	7
16	Seismic ground vibrations give advanced early-warning of subglacial floods. Nature Communications, 2020, 11, 2504.	5.8	18
17	Assessing the potential of passive seismic receiver functions for ore body exploration. Geophysical Prospecting, 2020, 68, 2094-2103.	1.0	1
18	The dynamics of a long-lasting effusive eruption modulated by Earth tides. Earth and Planetary Science Letters, 2020, 536, 116145.	1.8	13

#	Article	IF	CITATIONS
19	Estimating lateral and vertical resolution in receiver function data for shallow crust exploration. Geophysical Journal International, 2019, 218, 2045-2053.	1.0	4
20	SN-CAST: seismic network capability assessment software tool for regional networks-examples from Ireland. Journal of Seismology, 2019, 23, 493-504.	0.6	3
21	Tremor-rich shallow dyke formation followed by silent magma flow at Bárðarbunga in Iceland. Nature Geoscience, 2017, 10, 299-304.	5.4	36
22	Multiple coincident eruptive seismic tremor sources during the 2014–2015 eruption at Holuhraun, Iceland. Journal of Geophysical Research: Solid Earth, 2017, 122, 2972-2987.	1.4	27
23	Helicopter location and tracking using seismometer recordings. Geophysical Journal International, 2017, 209, 901-908.	1.0	13
24	Correlation of Wavefieldâ€5eparated Oceanâ€Generated Microseisms with North Atlantic Source Regions. Bulletin of the Seismological Society of America, 2016, 106, 1002-1010.	1.1	10
25	Seismic Noise Characterization in Proximity to Strong Microseism Sources in the Northeast Atlantic. Bulletin of the Seismological Society of America, 2016, 106, 464-477.	1.1	17
26	Relocation of longâ€period (LP) seismic events reveals en echelon fractures in the upper edifice of Turrialba volcano, Costa Rica. Geophysical Research Letters, 2016, 43, 10,105.	1.5	3
27	Micrometre-scale deformation observations reveal fundamental controls on geological rifting. Scientific Reports, 2016, 6, 36676.	1.6	11
28	New observations of displacement steps associated with volcano seismic longâ€period events, constrained by step table experiments. Geophysical Research Letters, 2015, 42, 3855-3862.	1.5	10
29	Amplitude and recurrence time analysis of LP activity at Mount Etna, Italy. Journal of Geophysical Research: Solid Earth, 2015, 120, 6474-6486.	1.4	11
30	A brittle failure model for longâ€period seismic events recorded at Turrialba Volcano, Costa Rica. Journal of Geophysical Research: Solid Earth, 2015, 120, 1452-1472.	1.4	14
31	Helicopter vs. volcanic tremor: Characteristic features of seismic harmonic tremor on volcanoes. Journal of Volcanology and Geothermal Research, 2015, 304, 108-117.	0.8	30
32	Segmented lateral dyke growth in a rifting event at Bárðarbunga volcanic system, Iceland. Nature, 2015, 517, 191-195.	13.7	436
33	Wave height quantification using land based seismic data with grammatical evolution. , 2014, , .		7
34	Persistent shallow background microseismicity on Hekla volcano, Iceland: A potential monitoring tool. Journal of Volcanology and Geothermal Research, 2014, 289, 224-237.	0.8	6
35	Long-period seismicity in the shallow volcanic edifice formed from slow-rupture earthquakes. Nature Geoscience, 2014, 7, 71-75.	5.4	132
36	Analysis of dynamics of vulcanian activity of Ubinas volcano, using multicomponent seismic antennas. Journal of Volcanology and Geothermal Research, 2014, 270, 35-52.	0.8	23

#	Article	IF	CITATIONS
37	Response of the San Jacinto Fault Zone to static stress changes from the 1992 Landers earthquake. Journal of Geophysical Research: Solid Earth, 2014, 119, 8914-8935.	1.4	10
38	Propagation of microseisms from the deep ocean to land. Geophysical Research Letters, 2014, 41, 6374-6379.	1.5	25
39	A passive lowâ€frequency seismic experiment in the Albertine Graben, Uganda. Geophysical Prospecting, 2013, 61, 39-61.	1.0	10
40	Moment tensor inversion for the source location and mechanism of long period (LP) seismic events from 2009 at Turrialba volcano, Costa Rica. Journal of Volcanology and Geothermal Research, 2013, 258, 215-223.	0.8	18
41	Origin of spurious single forces in the source mechanism of volcanic seismicity. Journal of Volcanology and Geothermal Research, 2013, 262, 1-6.	0.8	16
42	Investigating the source characteristics of long-period (LP) seismic events recorded on Piton de la Fournaise volcano, La Réunion. Journal of Volcanology and Geothermal Research, 2013, 258, 1-11.	0.8	13
43	Separation and location of microseism sources. Geophysical Research Letters, 2013, 40, 3118-3122.	1.5	7
44	Modelling fluid induced seismicity on a nearby active fault. Geophysical Journal International, 2013, 194, 1613-1624.	1.0	18
45	The coupling between very long period seismic events, volcanic tremor, and degassing rates at Mount Etna volcano. Journal of Geophysical Research: Solid Earth, 2013, 118, 4910-4921.	1.4	38
46	Eruptive fracture location forecasts from highâ€frequency events on Piton de la Fournaise Volcano. Geophysical Research Letters, 2013, 40, 4599-4603.	1.5	14
47	Source Separation on Seismic Data: Application in a Geophysical Setting. IEEE Signal Processing Magazine, 2012, 29, 16-28.	4.6	9
48	lmaging magma storage below Teide volcano (Tenerife) using scattered seismic wavefields. Geophysical Journal International, 2012, 191, 695-706.	1.0	14
49	A Lattice Boltzmann Method for Elastic Wave Propagation in a Poisson Solid. Bulletin of the Seismological Society of America, 2012, 102, 1224-1234.	1.1	15
50	Seismic swarms, fault plane solutions, and stress tensors for São Miguel Island central region (Azores). Journal of Seismology, 2012, 16, 389-407.	0.6	31
51	Time reverse location of seismic long-period events recorded on Mt Etna. Geophysical Journal International, 2011, 184, 452-462.	1.0	41
52	An irregular lattice method for elastic wave propagation. Geophysical Journal International, 2011, 187, 1699-1707.	1.0	19
53	Properties of the near-field term and its effect on polarisation analysis and source locations of long-period (LP) and very-long-period (VLP) seismic events at volcanoes. Journal of Volcanology and Geothermal Research, 2010, 192, 35-47.	0.8	32
54	Moment tensor inversion of explosive long period events recorded on Arenal volcano, Costa Rica, constrained by synthetic tests. Journal of Volcanology and Geothermal Research, 2010, 194, 189-200.	0.8	20

#	Article	IF	CITATIONS
55	Sub-basalt seismic imaging using optical-to-acoustic model building and wave equation datuming processing. Marine and Petroleum Geology, 2010, 27, 555-562.	1.5	7
56	Seasonal cycles of seismic velocity variations detected using coda wave interferometry at Fogo volcano, SA£o Miguel, Azores, during 2003–2004. Journal of Volcanology and Geothermal Research, 2009, 181, 231-246.	0.8	31
57	Volcano topography, structure and intrinsic attenuation: Their relative influences on a simulated 3D visco-elastic wavefield. Journal of Volcanology and Geothermal Research, 2009, 183, 122-136.	0.8	32
58	Dispersion analysis and computational efficiency of elastic lattice methods for seismic wave propagation. Computers and Geosciences, 2009, 35, 1768-1775.	2.0	21
59	Temporal changes in seismic wave propagation towards the end of the 2002 Mt Etna eruption. Geophysical Journal International, 2009, 178, 1779-1788.	1.0	7
60	Locating volcano-seismic signals in the presence of rough topography: wave simulations on Arenal volcano, Costa Rica. Geophysical Journal International, 2009, 179, 1547-1557.	1.0	13
61	Validation of elastic wave measurements of rock fracture compliance using numerical discrete particle simulations. Geophysical Prospecting, 2009, 57, 883-895.	1.0	20
62	Time reversal imaging of synthetic volcanic tremor sources. Geophysical Research Letters, 2009, 36, .	1.5	26
63	Source geometry from exceptionally high resolution long period event observations at Mt Etna during the 2008 eruption. Geophysical Research Letters, 2009, 36, .	1.5	31
64	Influence of nearâ€surface volcanic structure on longâ€period seismic signals and on moment tensor inversions: Simulated examples from Mount Etna. Journal of Geophysical Research, 2008, 113, .	3.3	82
65	Temporal evolution of long-period seismicity at Etna Volcano, Italy, and its relationships with the 2004–2005 eruption. Earth and Planetary Science Letters, 2008, 266, 205-220.	1.8	33
66	Momentâ€ŧensor inversion of LP events recorded on Etna in 2004 using constraints obtained from wave simulation tests. Geophysical Research Letters, 2007, 34, .	1.5	52
67	Analysis of sustained long-period activity at Etna Volcano, Italy. Journal of Volcanology and Geothermal Research, 2007, 160, 340-354.	0.8	49
68	Comment on "Diffusion of epicenters of earthquake aftershocks, Omori's law, and generalized continuous-time random walk models― Physical Review E, 2004, 69, 063101; discussion 063102.	0.8	2
69	A 3D discrete numerical elastic lattice method for seismic wave propagation in heterogeneous media with topography. Geophysical Research Letters, 2004, 31, .	1.5	77
70	Seismicity response to stress perturbations, analysed for a world-wide catalogue. Geophysical Journal International, 2003, 154, 179-195.	1.0	30
71	Numerical investigations of passive and reactive flow through generic single fractures with heterogeneous permeability. Earth and Planetary Science Letters, 2003, 213, 271-284.	1.8	31
72	A numerical study of passive transport through fault zones. Earth and Planetary Science Letters, 2003, 214, 633-643.	1.8	20

#	Article	IF	CITATIONS
73	Multifractal Modeling and Analyses of Crustal Heterogeneity. , 2003, , 207-236.		12
74	Interface scattering versus body scattering in subbasalt imaging and application of prestack wave equation datuming. Geophysics, 2002, 67, 1593-1601.	1.4	33
75	A comparison of published experimental data with a coupled lattice Boltzmann-analytic advection–diffusion method for reactive transport in porous media. Journal of Hydrology, 2002, 268, 143-157.	2.3	19
76	Fracture properties from seismic data – a numerical investigation. Geophysical Research Letters, 2002, 29, 9-1.	1.5	24
77	Effect of nonlinear surface interaction on seismic response of a fracture. , 2002, , .		Ο
78	Seismic image quality beneath strongly scattering structures and implications for lower crustal imaging: numerical simulations. Geophysical Journal International, 2001, 145, 423-435.	1.0	27
79	Sub-basalt imaging problems and the application of Artificial Neural Networks. Journal of Applied Geophysics, 2001, 48, 183-197.	0.9	4
80	Sub-basalt imaging using converted waves: numerical modelling. Geological Society Special Publication, 2001, 188, 223-235.	0.8	1
81	Numerical simulation of seismic waves using a discrete particle scheme. Geophysical Journal International, 2000, 141, 595-604.	1.0	89
82	Observation of diffusion processes in earthquake populations and implications for the predictability of seismicity systems. Journal of Geophysical Research, 2000, 105, 28081-28094.	3.3	52
83	Fracture-frequency prediction from borehole wireline logs using artificial neural networks. Geophysical Prospecting, 1999, 47, 1031-1044.	1.0	12
84	Multiscaling nature of sonic velocities and lithology in the upper crystalline crust: Evidence from the KTB main borehole. Geophysical Research Letters, 1999, 26, 275-278.	1.5	43
85	Statistical measures of crustal heterogeneity from reflection seismic data: The role of seismic bandwidth. Geophysical Research Letters, 1999, 26, 3241-3244.	1.5	24
86	Spatio-temporal analysis of stress diffusion in a mining-induced seismicity system. Geophysical Research Letters, 1999, 26, 3697-3700.	1.5	31
87	The broad-band fractal nature of heterogeneity in the upper crust from petrophysical logs. Geophysical Journal International, 1998, 132, 489-507.	1.0	107
88	Some remarks on the estimation of fractal scaling parameters from borehole wire-line logs. Geophysical Research Letters, 1997, 24, 1271-1274.	1.5	32
89	Coda wave imaging of the Long Valley Caldera using a spatial stacking technique. Geophysical Research Letters, 1997, 24, 1547-1550.	1.5	12
90	The use of a parallel virtual machine (PVM) for finite-difference wave simulations. Computers and Geosciences, 1997, 23, 771-783.	2.0	4

#	Article	IF	CITATIONS
91	Heterogeneity in a self-organized critical earthquake model. Geophysical Research Letters, 1996, 23, 383-386.	1.5	30
92	On the cause of 1/f-power spectral scaling in borehole sonic logs. Geophysical Research Letters, 1996, 23, 3119-3122.	1.5	34
93	The influence of non-regularly decaying coda wave envelopes upon the estimation of coda Q. Geophysical Research Letters, 1996, 23, 3087-3090.	1.5	1
94	Power-law random behaviour of seismic reflectivity in boreholes and its relationship to crustal deformation models. Earth and Planetary Science Letters, 1993, 117, 423-429.	1.8	8
95	An earthquake model with magnitudeâ€sensitive dynamics. Geophysical Research Letters, 1993, 20, 1403-1406.	1.5	6
96	Time and magnitude predictions in shocks due to chaotic fault interactions. Geophysical Research Letters, 1992, 19, 119-122.	1.5	24
97	A new look at the Rockall region, offshore Ireland. Marine and Petroleum Geology, 1991, 8, 410-416.	1.5	35
98	Evidence for chaotic behaviour in seismic wave scattering. Geophysical Research Letters, 1991, 18, 1901-1904.	1.5	15
99	P-wave sections in a realistic anisotropic lithosphere. Geophysical Journal International, 1991, 107, 709-714.	1.0	2
100	P-wave anisotropy in the lower lithosphere. Earth and Planetary Science Letters, 1990, 99, 58-65.	1.8	18
101	Full-Waveform based methods for Microseismic Monitoring Operations: an Application to Natural and Induced Seismicity in the Hengill Geothermal Area, Iceland. Advances in Geosciences, 0, 54, 129-136.	12.0	7